electronics

MDPI

Article

Preparation and Properties of Graphene Reinforced Copper Electrical Contact Materials for High-Voltage Direct Current Electrical Contacts

Liang Zhang [1,†], Qikai Ye [2,†], Xiangyu Zeng [3], Shuo Liu [4], Huaqiang Chen [5], Yingqi Tao [5], Xianwang Yu [5,*] and Xiaozhi Wang [4,*]

[1] Research Center for Humanoid Sensing and Perception, Zhejiang Lab, Hangzhou 311100, China; zhangliang3347@zhejianglab.com
[2] Carbon Nano New Energy Materials Research Center, Yongjiang Laboratory, Ningbo 315202, China; qikai-ye@ylab.ac.cn
[3] Hangzhou Institute of Technology, Xidian University, Hangzhou 311200, China; 21731052@zju.edu.cn
[4] School of Information and Electronic Engineering, Zhejiang University, Hangzhou 310027, China; 22131055@zju.edu.cn
[5] Green Energy New Material R & D Center, Zhejiang Metallurgical Research Institute Co., Ltd., Hangzhou 311500, China; shenwei@hzsteel.com (H.C.); taoyingqi@hzsteel.com (Y.T.)
* Correspondence: yuxianwang@hzsteel.com (X.Y.); xw224@zju.edu.cn (X.W.)
† These authors contributed equally to this work.

Abstract: With the rapid advancement of high-voltage engineering, meeting the increasingly demanding requirements for electrical contact materials in traditional high-voltage direct current (DC) contactors has become a challenge. Graphene has shown promise as an additive for enhancing the mechanical properties and functionality of reinforced polymers and ceramic matrix composites. However, its direct application in metal matrices remains challenging due to difficulties in achieving favorable wetting within carbon/metal systems, leading to inadequate dispersion of graphene and aggregation issues. In this study, we present an in situ growth method of graphene on copper powder. Employing a powder metallurgy approach, we have successfully established a continuous three-dimensional graphene interconnection network within the copper matrix. The resulting composite material not only exhibits elevated mechanical strength but also demonstrates slight improvements in conductivity and thermal conductivity. Notably, the prepared composite materials demonstrate exceptional performance in terms of friction resistance, oxidation resistance, and corrosion resistance, which are particularly suitable for applications such as electrical contact materials. These findings offer new possibilities for replacing traditional electrical contact materials in high-voltage DC contactors.

Keywords: graphene; composite material; CVD

Citation: Zhang, L.; Ye, Q.; Zeng, X.; Liu, S.; Chen, H.; Tao, Y.; Yu, X.; Wang, X. Preparation and Properties of Graphene Reinforced Copper Electrical Contact Materials for High-Voltage Direct Current Electrical Contacts. *Electronics* **2024**, *13*, 53. https://doi.org/10.3390/electronics13010053

Received: 15 November 2023
Revised: 12 December 2023
Accepted: 16 December 2023
Published: 21 December 2023

1. Introduction

The electric contactor is the core component of a direction current (DC) switch, serving as the carrier for current transmission and conversion. The quality and stability of its performance are crucial for the safe operation of the entire power and telecommunications system. Electrical contactors of power switches are submitted to huge thermal and mechanical stress, even more if in direct current, while performing disconnection of loads, isolation of circuits, and the clearing of electrical faults. During the operation of electric contacts, complex physical and chemical phenomena such as contact compression, mass transfer, welding, and arc erosion may occur [1]. With the development of the electric vehicle industry and the advent of the 5G communication era, the power demand has increased significantly, rendering the widely used copper chromium and copper tungsten contacts inadequate to meet the requirements [2–6]. Therefore, the development of high-power DC switches with stable performance has become urgent. With the advancement of vacuum

and gas-filled relays, such as ceramic-sealed gas-filled relays, rapid arc extinguishing can be achieved by utilizing inert gases, eliminating the need to consider the effects of oxidation. Currently, oxygen-free copper is commonly used as the contact material for high-voltage (60 V–1500 V) DC contactors due to its excellent electrical and thermal conductivity. However, it still faces issues such as arc ablation resistance and poor resistance to high-current impact. Improved dispersion-strengthened copper-based contacts involve various considerations in terms of processes, such as dispersion distribution and grain refinement. In order to enhance the wear resistance and arc ablation resistance of copper-based contact materials, the introduction of various fillers such as aluminum oxide (Al_2O_3), titanium oxide (TiO_2), W, Mo, Cr, tungsten carbide (WC), and titanium carbide (TiC) has been widely explored [4–6]. However, the addition of these fillers tends to reduce the electrical conductivity. Therefore, the challenge lies in improving the arc ablation resistance and wear resistance of oxygen-free copper while maintaining excellent conductivity.

Graphene, despite being composed only of carbon atoms (C), will be designated "Gr" in this manuscript; as a highly promising two-dimensional carbon material, it possesses an extremely large surface area. It exhibits advantages such as a carrier mobility of up to 15,000 $cm^2/(V{\cdot}s)$ and a thermal conductivity (TC) of up to 5150 $W/(m{\cdot}K)$, making it widely studied in the field of metal matrix composites, particularly in electrical contact materials [7–11]. The high carrier mobility of graphene and the high carrier density of metals can synergistically enhance conductivity, providing a rapid pathway for electron transport. This synergy contributes to maintaining or even elevating the electrical conductivity of composite materials. High TC is a good characteristic of electrical contact materials because it facilitates the conductor to dissipate the heat faster to cold areas. Considering the exceptional properties of graphene and its complementary effect with copper, using copper as the matrix and graphene as the filler in copper/graphene (Cu/Gr) alloy systems represents the most promising research direction for breaking through the performance barriers of traditional copper-based composites. However, the preparation of high-performance graphene-reinforced metal matrix composites still poses challenges due to the poor dispersion state of graphene in the matrix [12–15]. In previously published studies, in 2010, Xu Zhiping et al. investigated the properties of the interface between monolayer graphene and copper using first-principles calculations [16], and they found that the interfacial cohesive energy, strength, and electronic structure are closely related to their atomic geometries. Guo Junxian et al. employed the embedded atom method, reactive empirical bond-order potential, and Morse potential function to investigate the mechanical properties and related deformation mechanisms of graphene/copper composites for the first time using molecular dynamics [17]. The results indicated that the addition of graphene can simultaneously increase the elastic modulus and yield strength of the composite material. By comparing the expansion of initial microcracks over time in single-crystal copper and graphene-reinforced copper-based composites, it was found that the addition of graphene can significantly inhibit crack propagation. Additionally, the plasticity of the composite material is mainly derived from the slip of dislocations along the graphene surface, indicating the significant influence of the interfacial mechanical properties between graphene and copper on the overall performance of the composite material [10,18]. These theoretical studies collectively demonstrate that copper-graphene alloys exhibit excellent electrical and mechanical properties. However, in the majority of relevant research, the electrical conductivity of Cu/Gr composite materials is observed to decrease compared to pure copper [19,20]. This often results in poorer arc ablation resistance properties, rendering them unsuitable for applications in the high-voltage electrical contact materials field.

In this paper, we have developed a manufacturing strategy for high-performance advanced structural materials in the form of 3D graphene network/copper composites based on powder metallurgy. Utilizing the chemical vapor deposition (CVD) process, we grew graphene on pre-structured porous copper foams, followed by hot-pressing to produce Cu/Gr composites embedded with a uniform graphene network. The highly interconnected nature of the embedded graphene not only enhances the mechanical properties but

also significantly reduces electron scattering at the interface regions, establishing extensive conductive pathways for electron transport throughout the matrix. Compared to the powder mixing method, our approach enables the synthesis of well-crystallized graphene films, effectively addressing graphene's uniformity issues and enhancing interface binding. In contrast to the CVD growth process involving the use of isolating agents, our methodology significantly reduces production costs and eliminates post-treatment procedures such as acid washing. This streamlined process bodes well for the subsequent widespread applications and promotion of graphene-copper composite materials. Based on this composite material, we fabricated electrical contactors for high-voltage direct current switches and performed a comprehensive assessment of their electrical, thermal, mechanical, tribological (friction, wear, and lubrication) performance, arc ablation resistance properties, and electrical lifespan properties. Our work may further advance the commercial application of graphene-reinforced copper composites in the production of electrical contact elements.

2. Results and Discussion

The preparation process of the Cu/Gr composite material is illustrated in Figure 1a. Cu particles were subjected to thermal CVD to grow layers of graphene on their surfaces [21–23]. To ensure uniform growth, we made some modifications to the equipment, The specific modifications and process parameters can be found in the Methods. To ensure temperature stability in the heating zone, a three-chamber temperature control system was designed. In comparison to a single-chamber temperature control system, the three-chamber design balances temperature fluctuations across the entire system better, ensuring uniform graphene growth on the surface of copper powder. During the CVD growth process, no anti-sintering agent was added, resulting in the sintering of the sample into foam copper (Figure 1b). To verify the growth of graphene in foam copper, a small number of samples was taken and subjected to vacuum hot pressing, followed by immersion in ammonium persulfate for 12 h for etching. After the complete dissolution of the copper, the solution turned blue, leaving behind a black graphite sponge (Figure 1c and its illustration). The prepared Cu/Gr alloy exhibited interconnected graphene networks on the Cu phase, forming a complete graphene network. The average size of the Cu particles before and after graphene growth (60 μm) showed no significant change, as shown in Figure 1d–g. However, the surface of the copper particles coated with graphene appeared significantly smoother, which can be attributed to the surface recrystallization of copper particles during the high-temperature process. Figure 1h is a schematic diagram of the crystal structure of graphene. To demonstrate the uniformity of graphene growth in each part of the quartz mold, samples from the upper, middle, and lower regions were selected for Raman spectrum testing. The Raman spectrum of the Cu/Gr composite is depicted in Figure 1i. The low intensity of the D peak near 1300 cm^{-1} indicates that the prepared graphene had fewer defects [24]. The G-band in the spectral range of 1579–1588 cm^{-1} is associated with the stretching-vibration mode of the sp^2 sites, including C=C bonds found in aromatic compounds [25–27]. Conversely, the 2D band, positioned between 2688 and 2699 cm^{-1}, originates from a double-resonance process. The ratio of I_{2D}/I_G is used to describe the degree of sp^2 hybridization in the C=C bonds of graphene layers, which is often employed to determine the number of graphene layers [27–29]. The test results indicated that the graphene prepared by CVD technology exhibited a multi-layer structure, and the number of layers of graphene on the surface and bottom of the sample was approximately the same.

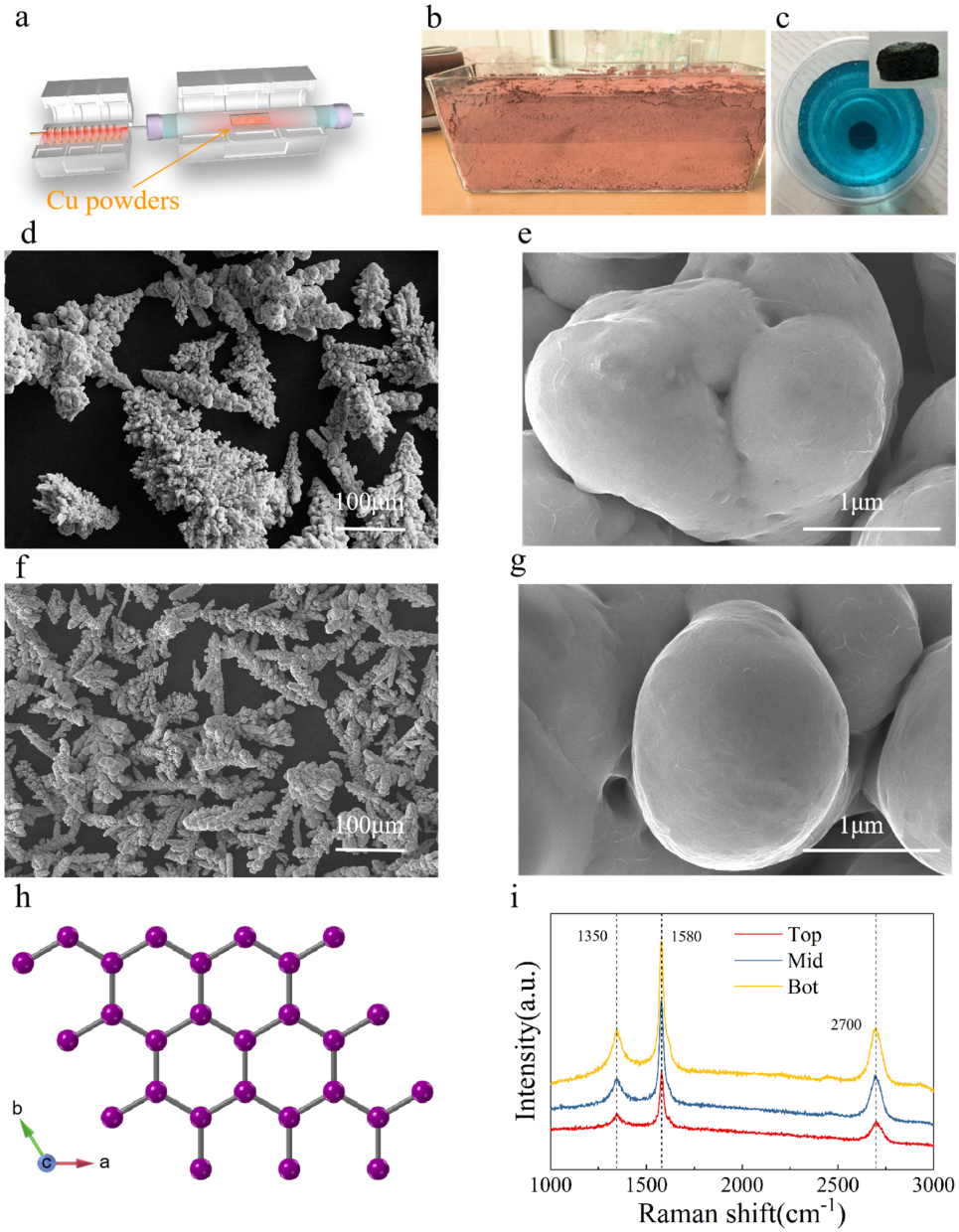

Figure 1. (**a**) Process diagram of in situ growth of graphene on the surface of copper powder by thermal CVD. (**b**) An image of the Cu-Gr composites captured by a high-resolution camera. (**c**) Cu-Gr composites etched by ammonium persulfate. Inset, remaining graphene 3D network after etching. (**d**,**e**) SEM images of Cu. (**f**,**g**) SEM images of Cu-Gr composites. (**h**) Schematic diagram of the crystal structure of graphene. (**i**) Raman spectra of three different positions of Cu-Gr composites in the mold.

Next, a series of tests and evaluations were conducted on the comprehensive properties of the prepared copper graphene alloy, comparing it with oxygen-free copper. The graphene network, uniformly distributed within the composite, enhances its properties by inhibiting dislocation movement and improving hardness. Mechanical and processing properties are crucial for high-quality electrical contact materials. The tensile testing results of the composite materials are presented in Figure 2a, demonstrating an improvement in tensile strength compared to pure copper, albeit with a slight decrease in ductility. To evaluate the tribological properties of Cu/Gr composites, a Sliding Friction Wear Tester M200 (ZHDLYQ, Beijing, China) was employed according to the standard GB/T 12444-2006 [30]. Figure 2b illustrates a reduction in the friction coefficient of the Cu/Gr composite material to 0.3, which is 38% lower than that of oxygen-free copper. The wear rate of the composite

material is depicted in Figure 2c, indicating a decrease to 2×10^{-5} $mm^3/(N \cdot m)^3$, which is approximately 67% lower than that of oxygen-free copper. The interlayers of multilayer graphene are weakly bound by van der Waals forces. During wear, under shear forces, these layers tend to form slip planes along the plane, thereby transforming the original wear behavior from metal–metal contact to interactions between graphene slip planes. This transition inhibits adhesive wear, consequently reducing both friction coefficient and wear rate. Excellent electrical conductivity and thermal conductivity are fundamental requirements for electrical contact materials in ultra-high-voltage DC contactors, ensuring rapid heat dissipation during operation. Figure 2d illustrates a comparison between the conductivity and thermal conductivity of the Cu/Gr composite material and oxygen-free copper. The thermal conductivity test was performed using a laser thermal conductivity tester (LFA-467, Netzsch, Selb, Germany) at room temperature, while the conductivity was measured using a DC resistance tester. The test results indicate slight improvements in conductivity and thermal conductivity compared to oxygen-free copper, overcoming the traditional alloy limitations of conflicting mechanical and electrical properties. These enhancements are attributed to the complete 3D interconnection network formed by graphene within the alloy. Undoubtedly, as electrical contact materials for ultra-high-voltage DC contactors, Cu/Gr composite materials exhibit enhanced resistance to arc erosion due to their excellent conductivity and heat transfer capabilities. Figure 2e displays the thermogravimetric (TG) analysis and micro quotient thermogravimetric (DTG) analysis curves. Noticeably, the oxidation resistance of the composite material is significantly improved between 400 °C and 800 °C due to the blocking effect of the graphene network, which prevents oxygen from contacting the copper. The thermal expansion coefficient test of the composite materials is shown in Figure 2f. As expected, the in situ growth process yields a significantly reduced thermal expansion coefficient, as graphene possesses a small thermal expansion coefficient, and the complete graphene interconnection network tightly encloses copper particles, restricting thermal expansion. Conversely, the composite prepared by the traditional mixing process exhibits a thermal expansion coefficient nearly identical to that of oxygen-free copper due to the uneven dispersion of graphene, the lack of a complete network, and its inability to bind copper's thermal expansion.

The frictional properties of Cu/Gr composite materials were further evaluated using Rtec's MFT-5000 (Rtec, San Jose, CA, USA) multifunctional friction and wear tester and the Rtec UP-Dule Mode white-light interference 3D surface profiler (Rtec, USA). Oxygen-free Cu and Cu/Gr composite materials were subjected to wear tests against tungsten carbide balls under the same experimental parameters, and the three-dimensional surface morphology of the wear tracks is presented in Figure 3a,d. Figure 3b,e show the roughness profiles along the horizontal friction direction, revealing that the lengths of the wear craters for both samples along the friction direction are similar, but the depth of the craters in the Cu/Gr composite material is significantly shallower. Figure 3c,f display the roughness profiles along the vertical friction direction, where both the depth and width of the craters in the Cu/Gr composite material are smaller obviously. This could be attributed to the graphene network preventing copper from diffusing laterally during the friction process. Figure S1a,b depict 3D images from confocal microscope images; Figure S1c,d show the projected views of the wear craters, and Table S1 shows calculation data of wear craters. It can be observed that the wear area (0.4870 mm^2) and maximum wear depth (4.335 μm) of the Cu/Gr composite materials are noticeably less than those of oxygen-free copper (wear area: 0.8591 mm^2, maximum wear depth: 8.251 μm). This is because the graphene, grown in situ on the copper powder surface through the CVD process, forms a uniform continuous network in the Cu/Gr alloy, resulting in excellent self-lubrication and enhanced wear resistance of the composite material. Additionally, the hardness of the Cu/Gr composite material (70 HB) is higher than that of oxygen-free copper (56 HB). In summary, the comprehensive testing and characterization results indicate that both the mechanical and the frictional properties of the Cu/Gr composite material have been improved.

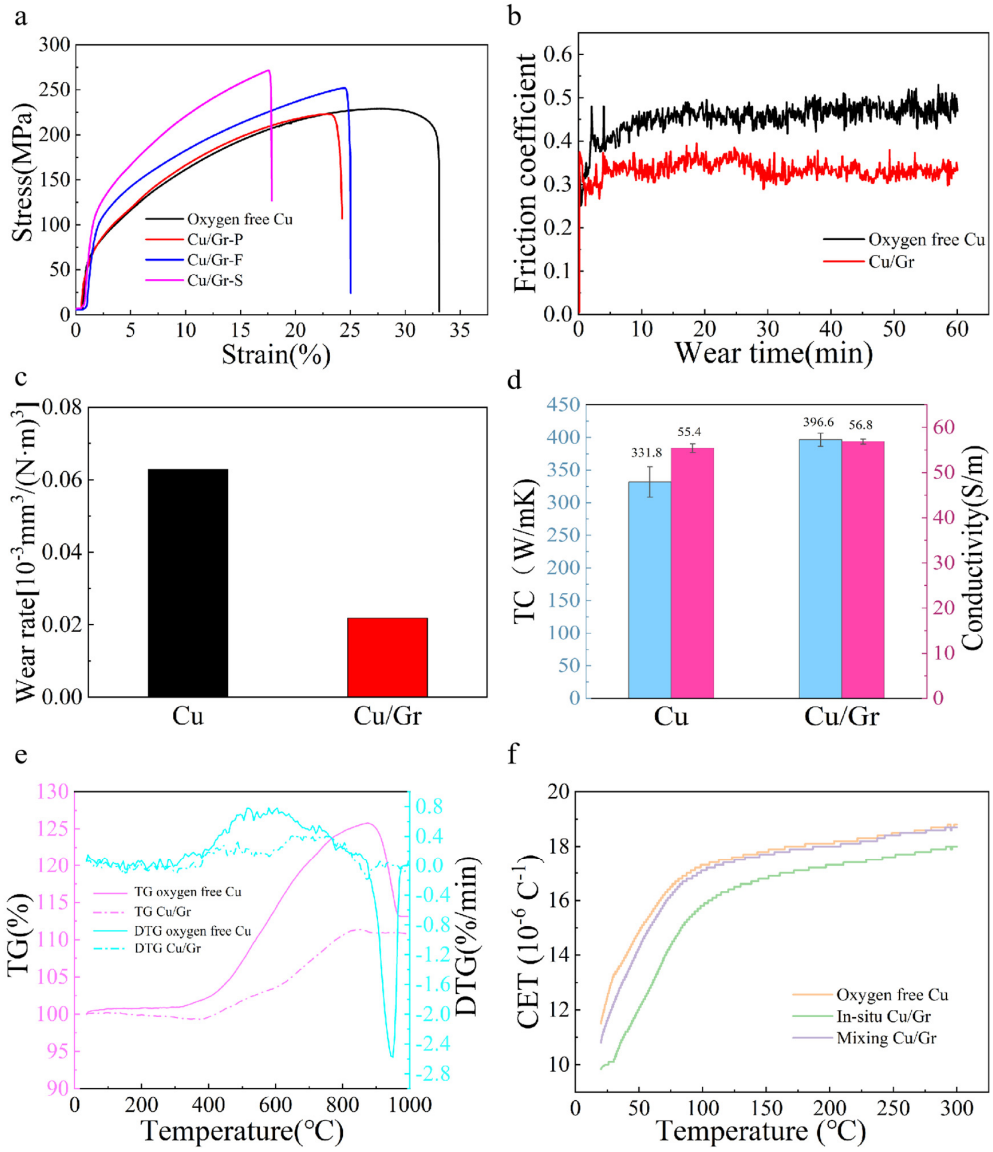

Figure 2. (**a**) Comparison of the tensile stress–strain curve of different composites with that of oxygen-free Cu. (**b**) Friction coefficients of the Cu-Gr composites and oxygen-free copper varied with sliding time. (**c**) Wear rate of the Cu-Gr composites and oxygen-free copper. (**d**) Conductivity and thermal conductivity of the Cu-Gr composites and oxygen-free Cu (**e**) TG and DTG analysis of the Cu-Gr composites and oxygen-free copper (**f**) Thermal expansion coefficients of the in situ Cu-Gr composites, mixing Cu-Gr composites, and oxygen-free copper.

In high-power DC switches, the arc ablation resistance property is of paramount importance. To evaluate the arc ablation resistance property of Cu/Gr composite materials, the electrical lifetimes of the samples were tested at operating voltages of 400 V and 750 V using the PAT500 high-voltage DC power testing system (CETC, Heifei, China) at the Fortieth Research Institute of China Electronics Technology Group Corporation. Figure 4a illustrates the prepared static and dynamic contact parts. Figure 4b demonstrates the electrical lifetimes of Cu/Gr composite materials and compares them with those of oxygen-free copper electrical contacts processed under the same conditions. Notably, under both 400 V and 750 V conditions, Cu/Gr composite materials exhibited significantly extended electrical lifetimes compared to oxygen-free copper electrical contacts. This observation underscores the superior arc ablation resistance property of Cu/Gr composite materials. Figure 4c–f depict SEM and confocal microscopy images of the contact surfaces of the two kinds of electrical contact samples after arc breakdown.

These images reveal that Cu/Gr composite materials exhibit less pronounced surface irregularities resulting from arc breakdown. These results can be mainly attributed to the following aspects. Firstly, graphene exhibits a lower work function than copper, which to a certain extent suppresses electron emission during arc breakdown. Secondly, its outstanding electrical and thermal conductivity aids in rapidly dissipating arc energy during arc ablation, preventing significant charge accumulation. This manifests macroscopically by restraining contact temperature rise and minimizing surface erosion due to the arc. Finally, the three-dimensional network structure of graphene separates the copper matrix into discrete crystalline "micro-cells", wherein the graphene isolation layers inhibit copper splattering during arc action, restraining further copper ablation. Consequently, the macroscopic manifestation within the ablation region of Cu/Gr composite materials appears as smaller isolated ablation pits. The findings conclusively demonstrate that under both 400 V and 750 V operating voltages, Cu/Gr composite materials exhibit outstanding arc ablation resistance properties and prolonged electrical lifetimes.

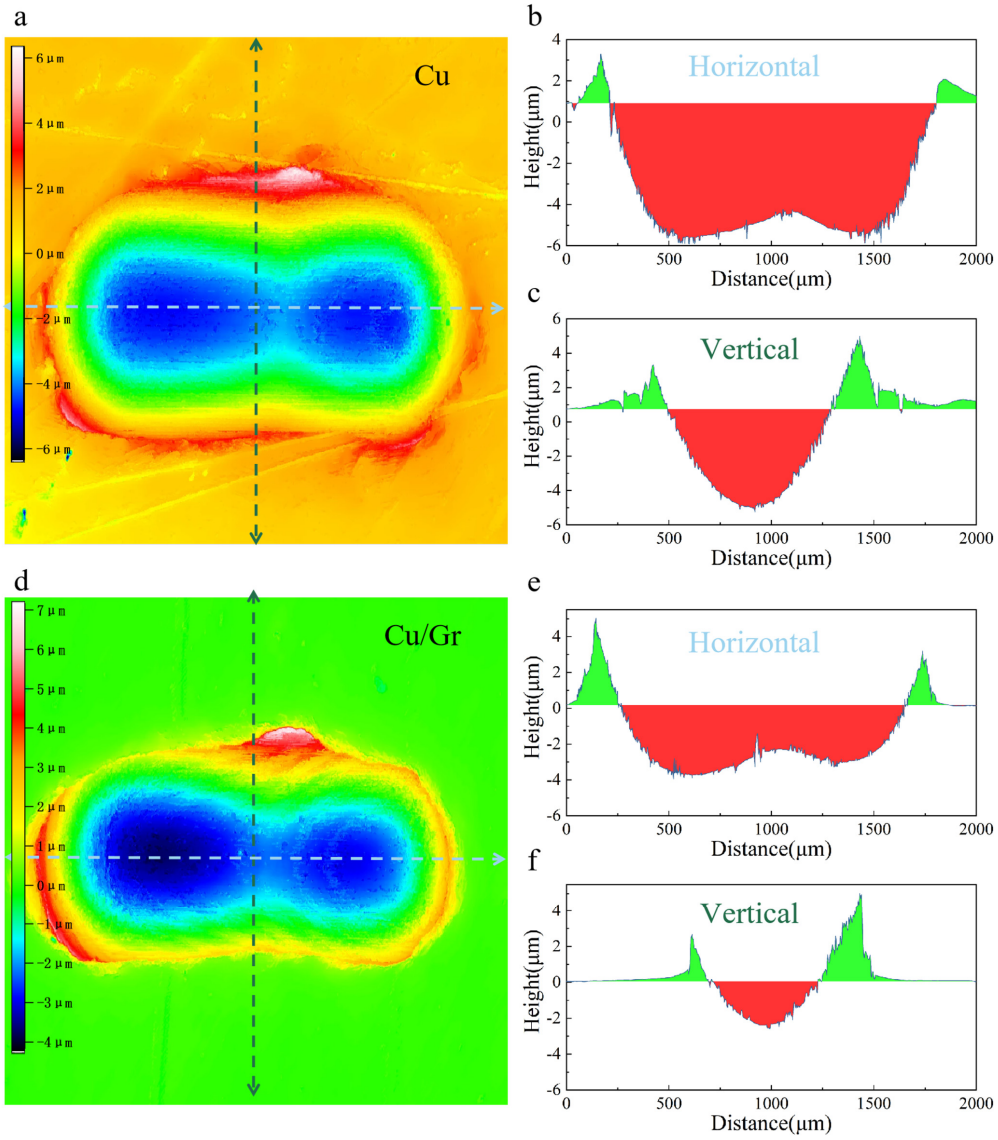

Figure 3. (**a**) Three-dimensional surface morphology of oxygen-free Cu. (**b**,**c**) The wear tracks profiles of oxygen-free Cu in horizontal and vertical directions, respectively. The green and red filled areas in figures represent above and below the sample surface, respectively. (**d**) Three-dimensional surface morphology of Cu/Gr. (**e**,**f**) The wear tracks profiles of Cu/Gr in horizontal and vertical directions, respectively. The green and red filled areas in figures represent above and below the sample surface, respectively.

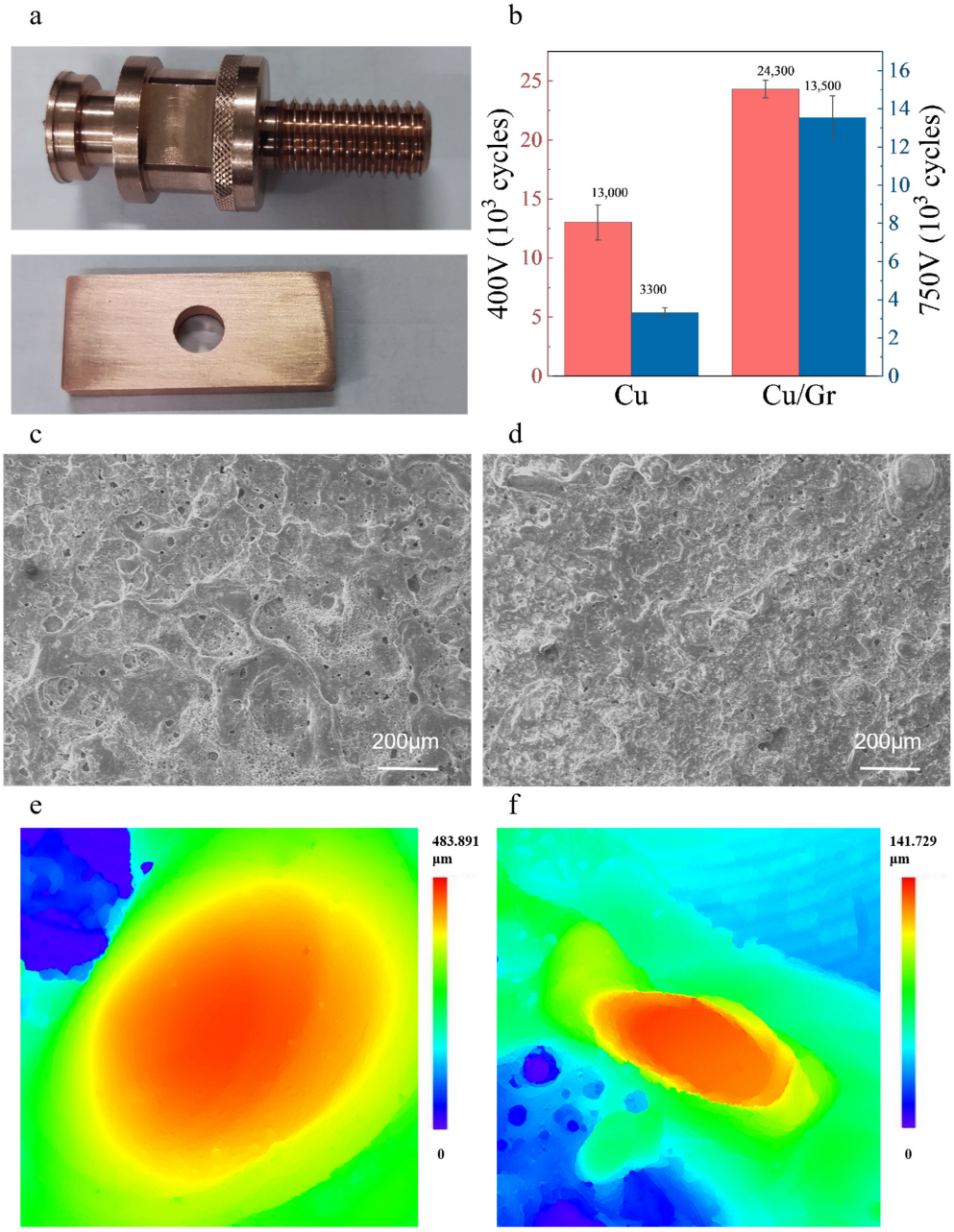

Figure 4. (**a**) Photos of static and dynamic contacts prepared using Cu/Gr composite materials. (**b**) Statistics of the average electrical life of two types of electrical contacts at 400 V and 750 V, respectively. (**c**) Surface SEM images of oxygen-free Cu contacts after arc breakdown. (**d**) Surface SEM images of Cu/Gr composite contacts after arc breakdown. (**e**) Three-dimensional surface morphology of oxygen-free Cu contacts after arc breakdown. (**f**) Three-dimensional surface morphology of Cu/Gr composite contacts after arc breakdown.

3. Conclusions

In summary, we have developed a manufacturing strategy for high-performance advanced structural materials in the form of 3D graphene network/copper composites based on powder metallurgy. This approach involves directly wrapping graphene around copper particles, effectively addressing the challenges associated with graphene dispersion and resulting in the fabrication of high-performance copper-graphene alloys. Multilayer graphene grown via CVD forms an interconnected 3D network framework within the composite material through powder metallurgy and hot-pressing processes, offering protection to the copper particles and thereby enhancing the mechanical and tribological properties of the

composite material. The graphene network also provides pathways for electron transport, effectively retaining the inherent advantages of high electrical and thermal conductivity in oxygen-free copper. Notably, the high-voltage electrical contact materials prepared using these composite materials exhibit extended electrical lifetime and improved arc ablation resistance compared to pure copper. Our work introduces a novel approach to designing advanced high-voltage electrical contact materials, offering advantages such as low cost and high robustness. The Cu/Gr composite material contactors hold promising applications in the electric vehicle domain, particularly in the process of DC fast charging. The control of high current flow interruption and connection necessitates the utilization of DC contactors, where the contact material stands as a pivotal component, emphasizing the paramount importance of its performance reliability. The process route described in this paper embodies scalability and cost-effectiveness, showcasing significant market potential.

Methods

Materials. The Cu powders were provided by Zhejiang Metallurgical Research Institute Co., Ltd., Hangzhou, China. Methane and argon gas were purchased from Hangzhou Bestgas Co., Ltd., Hangzhou, China. All reagents were used without further purification.

CVD equipment modification. To achieve uniform deposition of graphene on the surface of stacked powder, certain modifications were made to the CVD equipment (Figure S2). In the design, to enhance the reactivity of the reaction gas, an activation process was introduced by using a preheating furnace unit. Typically, the preheating furnace unit is positioned at the front end of the reaction chamber, and the gas mixture is preheated to the appropriate reaction temperature before its cracking. In the design of the preheating module structure, a helical copper tube was employed as the gas transport conduit. This serves to promote the diffusion and dissolution of gas molecules on one hand and, on the other hand, leverages copper as a catalyst to enhance the reactivity of carbon source gases (such as methane and acetylene). As the gas passes through the long spiral tube, the diffusion motion effectively promotes the mixing of the three gas supply branch gases, ensuring the stability of the gas ratio transported into the reaction chamber. This prevents fluctuations in real-time gas ratio due to different gas diffusion rates, which is advantageous for the stability of the graphene growth process. Additionally, under preheating conditions, copper plays a role in promoting the dissociation and reaction of methane and hydrogen, converting these gases into activated state molecules and enhancing their reactivity.

CVD growth of graphene on Cu powder. Place a quartz boat loaded with copper powder into the heating chamber, purge with 200 sccm of Ar for 5 min to remove air, and then heat at a rate of 15 °C/min to 1000 °C in a mixed atmosphere of 160 sccm of H_2 and 500 sccm of Ar (with a preheat chamber temperature of 200 °C). After temperature stabilization, introduce 30 sccm of CH_4, maintain for 120 min, and then turn off the CH_4 and H_2, allowing natural cooling to room temperature.

Powder metallurgical process for processing Cu/Gr composite. The prepared foam Cu/Gr structural composite block was formed into a high-density block through a process involving pressing, sintering, re-pressing, re-sintering, and hot extrusion. Prior to pressing and sintering, the foam Cu/Gr was machined to adapt to the pressing mold, preventing excessive porosity that could lead to pressing cracks. The pressing pressure applied was 200 MPa. After depressurization, the block was removed from the mold, resulting in a blank of the required shape. This blank was placed in a high-temperature sintering furnace for dense sintering in a vacuum or inert gas atmosphere. A hybrid sintering method involving both vacuum and inert gas pressure was employed to remove internal gases from the blank as much as possible. The temperature was initially raised to 800 °C under vacuum conditions, followed by pressurization with inert gas. The heating rate was then gradually increased to 1000 °C, maintained for 30 min, and then followed by additional sintering for 60 min under vacuum conditions. This process yielded a sintered block. To further densify the block, it was subjected to a re-pressing and re-sintering process. Subsequently, the block was placed in a hot extrusion device, and at 650 °C, it was extruded at a speed of 10 mm/s to obtain the final composite block.

Characterization techniques. Raman spectroscopy (Thermo Fischer DXR, Waltham, MA, USA) with a 532 nm laser was performed to characterize the graphene materials. Scanning electron microscopy (HITACHI SU8010, Tokyo, Japan) was used to observe the microstructures of the powders and composites.

Electrical conductivity measurements. Electrical conductivity was tested by a DC resistance tester PC36C (Sulei, Shanghai, China), and all the samples had a diameter of 0.5 mm and were surface polished.

Thermal properties measurement. The thermal conductivity of the samples was measured using the laser flash analysis method on the Netzsch LFA 467 Nano Flash apparatus (Netzsch, Germany). Additionally, the samples were subjected to TG and DTG analyses using the Netzsch STA449F5 (Netzsch, Germany) simultaneous thermal analyzer. The thermal expansion coefficient test was conducted using a DIL 402CL thermal expansion coefficient instrument (Netzsch, Germany).

Mechanical properties measurement. For static tensile testing, the obtained bulk samples were cut and polished into dog-bone shapes. Tensile tests were conducted using a computer-controlled electronic universal testing machine WDW-100E (SDSF, Jinan, China).

Supplementary Materials: The following supporting information can be downloaded at: https://www.mdpi.com/article/10.3390/electronics13010053/s1, Figure S1. (a) Confocal microscopic 3D images of oxygen free Cu. (b) Confocal microscopic 3D images of Cu/Gr composite. (c) The projected views of the wear craters of oxygen free Cu. (d) The projected views of the wear craters of Cu/Gr composite. Figure S2. Image of high-voltage DC contactor sample for testing. Table S1. Calculation data of wear craters projection for oxygen free Cu and Cu/Gr composite.

Author Contributions: L.Z.: conceptualization, data curation, writing—review and editing, writing—original draft, investigation, formal analysis, methodology, software, validation, visualization, and writing and revising the manuscript. Q.Y.: conceptualization, writing—review and editing, and data texting; performed the experiments and conceived the idea. X.Z., S.L., H.C. and Y.T.: investigation. X.Y. and X.W.: projector administration and funding acquisition. All authors have read and agreed to the published version of the manuscript.

Funding: This research was funded by the "Pioneer" and "Leading Goose" R&D Program of Zhejiang (2022C01141) by Yingqi Tao.

Data Availability Statement: The data that support the findings of this study are available from the corresponding authors upon reasonable request.

Conflicts of Interest: The authors declare no competing financial interest. The funding sponsors had no role in the design of the study; in the collection, analyses, or interpretation of data; in the writing of the manuscript, and in the decision to publish the results.

References

1. Zhang, X.; Zhang, Y.; Tian, B.; Jia, Y.; Fu, M.; Liu, Y.; Song, K.; Volinsky, A.A.; Yang, X.; Sun, H. Graphene oxide effects on the properties of Al_2O_3-Cu/$_{35}W_5Cr$ composite. *J. Mater. Sci. Technol.* **2020**, *37*, 185–199. [CrossRef]
2. Chen, W.; Shi, Y.; Dong, L.; Wang, L.; Li, H.; Fu, Y. Infiltration sintering of WCu alloys from copper-coated tungsten composite powders for superior mechanical properties and arc-ablation resistance. *J. Alloys Compd.* **2017**, *728*, 196–205. [CrossRef]
3. Dong, L.; Chen, W.; Zheng, C.; Deng, N. Microstructure and properties characterization of tungsten–copper composite materials doped with graphene. *J. Alloys Compd.* **2017**, *695*, 1637–1646. [CrossRef]
4. Franck, C.M. HVDC circuit breakers: A review identifying future research needs. *IEEE Trans. Power Deliv.* **2011**, *26*, 998–1007. [CrossRef]
5. Xu, L.; Srinivasakannan, C.; Zhang, L.; Yan, M.; Peng, J.; Xia, H.; Guo, S. Fabrication of tungsten–copper alloys by microwave hot pressing sintering. *J. Alloys Compd.* **2016**, *658*, 23–28. [CrossRef]
6. Yu, L.; Wang, J.; Geng, Y.; Kong, G.; Liu, Z. High-current vacuum arc phenomena of nanocrystalline $CuCr_{25}$ contact material. *IEEE Trans. Plasma Sci.* **2011**, *39*, 1418–1426.
7. Novoselov, K.S.; Fal'ko, V.I.; Colombo, L.; Gellert, P.R.; Schwab, M.G.; Kim, K. A roadmap for graphene. *Nature* **2012**, *490*, 192–200. [CrossRef]
8. Novoselov, K.S.; Geim, A.K.; Morozov, S.V.; Jiang, D.-E.; Zhang, Y.; Dubonos, S.V.; Grigorieva, I.V.; Firsov, A.A. Electric field effect in atomically thin carbon films. *Science* **2004**, *306*, 666–669. [CrossRef]
9. Geim, A.K.; Novoselov, K.S. The rise of graphene. *Nat. Mater.* **2007**, *6*, 183–191. [CrossRef]

10. Kim, Y.; Lee, J.; Yeom, M.S.; Shin, J.W.; Kim, H.; Cui, Y.; Kysar, J.W.; Hone, J.; Jung, Y.; Jeon, S. Strengthening effect of single-atomic-layer graphene in metal–graphene nanolayered composites. *Nat. Commun.* **2013**, *4*, 2114. [CrossRef]
11. Zhang, Y.; Gomez, L.; Ishikawa, F.N.; Madaria, A.; Ryu, K.; Wang, C.; Badmaev, A.; Zhou, C. Comparison of graphene growth on single-crystalline and polycrystalline Ni by chemical vapor deposition. *J. Phys. Chem. Lett.* **2010**, *1*, 3101–3107. [CrossRef]
12. Picot, O.T.; Rocha, V.G.; Ferraro, C.; Ni, N.; D'elia, E.; Meille, S.; Chevalier, J.; Saunders, T.; Peijs, T.; Reece, M.J. Using graphene networks to build bioinspired self-monitoring ceramics. *Nat. Commun.* **2017**, *8*, 14425. [CrossRef] [PubMed]
13. Shahil, K.M.; Balandin, A.A. Graphene–multilayer graphene nanocomposites as highly efficient thermal interface materials. *Nano Lett.* **2012**, *12*, 861–867. [CrossRef] [PubMed]
14. Yolshina, L.A.; Muradymov, R.V.; Korsun, I.V.; Yakovlev, G.A.; Smirnov, S.V. Novel aluminum-graphene and aluminum-graphite metallic composite materials: Synthesis and properties. *J. Alloys Compd.* **2016**, *663*, 449–459. [CrossRef]
15. Hang, L.; Zhao, Y.; Zhang, H.; Liu, G.; Cai, W.; Li, Y.; Qu, L. Copper nanoparticle@ graphene composite arrays and their enhanced catalytic performance. *Acta Mater.* **2016**, *105*, 59–67. [CrossRef]
16. Xu, Z.; Buehler, M.J. Interface structure and mechanics between graphene and metal substrates: A first-principles study. *J. Phys. Condens. Matter.* **2010**, *22*, 485301. [CrossRef]
17. Guo, J.; Wang, B.; Yang, Z. Molecular dynamics simulations on the mechanical properties of graphene/Cu composites. *Acta Mater. Compos. Sin.* **2014**, *31*, 152–157.
18. Xiong, D.-B.; Cao, M.; Guo, Q.; Tan, Z.; Fan, G.; Li, Z.; Zhang, D. Graphene-and-copper artificial nacre fabricated by a preform impregnation process: Bioinspired strategy for strengthening-toughening of metal matrix composite. *ACS Nano* **2015**, *9*, 6934–6943. [CrossRef]
19. Li, X.; Yan, S.; Chen, X.; Hong, Q.; Wang, N. Microstructure and mechanical properties of graphene-reinforced copper matrix composites prepared by in-situ CVD, ball-milling, and spark plasma sintering. *J. Alloys Compd.* **2020**, *834*, 155182. [CrossRef]
20. Hidalgo-Manrique, P.; Lei, X.; Xu, R.; Zhou, M.; Kinloch, I.A.; Young, R.J. Copper/graphene composites: A review. *J. Mater. Sci.* **2019**, *54*, 12236–12289. [CrossRef]
21. Wu, M.; Hou, B.; Shu, S.; Li, A.; Geng, Q.; Li, H.; Shi, Y.; Yang, M.; Du, S.; Wang, J.-Q. High oxidation resistance of CVD graphene-reinforced copper matrix composites. *Nanomaterials* **2019**, *9*, 498. [CrossRef] [PubMed]
22. Xiao, Q.; Yi, X.; Jiang, B.; Qin, Z.; Hu, J.; Jiang, Y.; Liu, H.; Wang, B.; Yi, D. In-situ synthesis of graphene on surface of copper powder by rotary CVD and its application in fabrication of reinforced Cu-matrix composites. *Adv. Mater. Sci.* **2017**, *2*, 1–6. [CrossRef]
23. Chen, Y.; Zhang, X.; Liu, E.; He, C.; Han, Y.; Li, Q.; Nash, P.; Zhao, N. Fabrication of three-dimensional graphene/Cu composite by in-situ CVD and its strengthening mechanism. *J. Alloys Compd.* **2016**, *688*, 69–76. [CrossRef]
24. Ferrari, A.C.; Basko, D.M. Raman spectroscopy as a versatile tool for studying the properties of graphene. *Nat. Nanotechnol.* **2013**, *8*, 235–246. [CrossRef] [PubMed]
25. Ferrari, A.C.; Robertson, J. Interpretation of Raman spectra of disordered and amorphous carbon. *Phys. Rev. B* **2000**, *61*, 14095. [CrossRef]
26. Gupta, A.; Chen, G.; Joshi, P.; Tadigadapa, S. Eklund, Raman scattering from high-frequency phonons in supported n-graphene layer films. *Nano Lett.* **2006**, *6*, 2667–2673. [CrossRef] [PubMed]
27. Ferrari, A.C.; Meyer, J.C.; Scardaci, V.; Casiraghi, C.; Lazzeri, M.; Mauri, F.; Piscanec, S.; Jiang, D.; Novoselov, K.S.; Roth, S. Raman spectrum of graphene and graphene layers. *Phys. Rev. Lett.* **2006**, *97*, 187401. [CrossRef]
28. Malard, L.M.; Pimenta, M.A.; Dresselhaus, G.; Dresselhaus, M.S. Raman spectroscopy in graphene. *Phys. Rep.* **2009**, *473*, 51–87. [CrossRef]
29. Robertson, A.W.; Warner, J.H. Hexagonal single crystal domains of few-layer graphene on copper foils. *Nano Lett.* **2011**, *11*, 1182–1189. [CrossRef]
30. *GB/T 12444-2006*; Metallic Materials—Wear Test Method-Block-on-Ring Sliding Wear Test. Standardization Administration of the People's Republic of China: Beijing, China, 2006.